Supporting Information

Direct particle tracking observation and Brownian dynamics simulations of a single nanoparticle optically trapped by a plasmonic nanoaperture

Zhe Xu,[†] *Wuzhou Song,*[†,‡] *and Kenneth B. Crozier**[*,†,§]

[†]School of Physics, University of Melbourne, Victoria 3010, Australia

[‡]School of Materials Science and Engineering, Huazhong University of Science and Technology, Wuhan 430074, P. R. China

[§]Department of Electrical and Electronic Engineering, University of Melbourne, Victoria 3010, Australia

Corresponding Author

* E-mail: kcrozier@unimelb.edu.au.

S1 Experimental setup

The experimental set-up is schematically illustrated as Fig. S1a. Trapping is monitored by observing the nanoparticle (NP) fluorescence using an electron multiplying camera (EM-CCD). An optical beam shutter is used to switch on and off the trapping laser. A 1064 nm half-wave plate is used to rotate the polarization of the laser beam (*x*-polarized). The polystyrene nanoparticles (FluoSpheres, 20 nm diameter, carboxylate-modified, Nile Red, Life Technologies) are suspended in Ultra-Pure distilled water with a trace amount of Tween 20 surfactant (0.05% v/v) and the solution is passed through a filter to remove aggregates, etc. The nanoparticles have a coefficient of variation of about 20%, according to the manufacturer (Life Technologies). The transmission of oil objective to the focal plane at 1064 nm is ~50%. Fig. S1b details the cross section of closed perfusion chamber, sealed with UV-cured optical adhesives. The chamber is fabricated on a glass slide using standard photolithography methods. The photoresist (AZ9260) thickness is determined by the rotation speed of spin-coater and measured with an optical profilometer. A thickness of ~20 μm is chosen in order to make the chamber relatively shallow, which facilitates observation of the trapping process. The sample package is mounted upside-down. Polyethylene tubing is used to deliver fluid into the channel. Prior to chamber fabrication, the glass coverslip is sonicated in water and cleaned with a plasma cleaner to remove particles etc. from the surface. The gold film (containing the DNH) is washed with acetone and rinsed with isopropanol and distilled water. Fig. S1c shows the SEM (left) and microscope (right) images of double nanohole (DNH) aperture fabricated in the gold film.

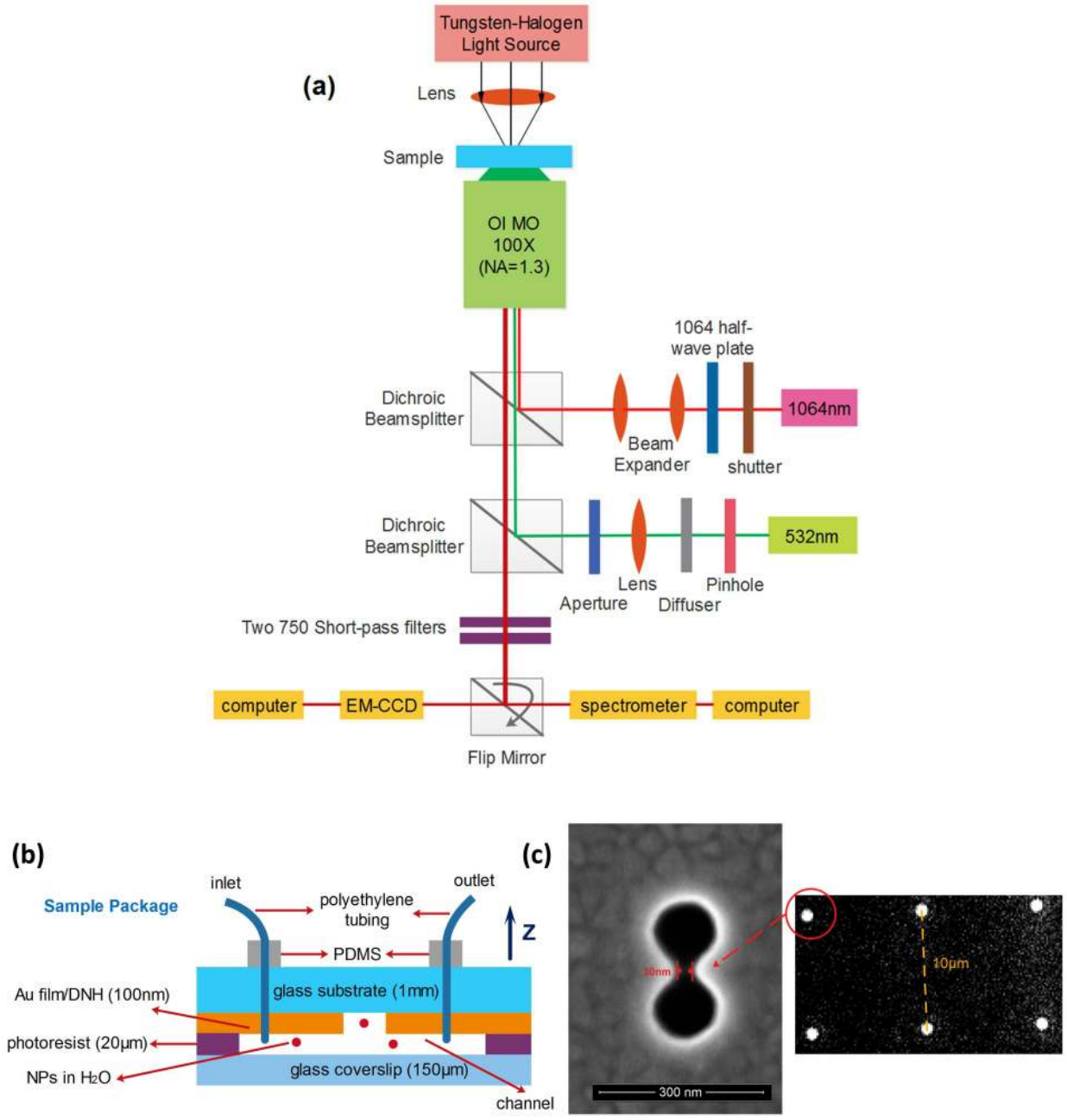

Figure S1. (a) Schematic diagram of experimental set-up. Trapping laser: Laser Quantum Ventus 1064; Oil immersion objective: Nikon Plan Fluorite Oil Immersion Objective, 100×, NA=1.3; Electron multiplying camera: EM-CCD, ProEM-HS: 512×512. (b) Cross section of closed perfusion chamber, sealed with UV-cured optical adhesives. (c) SEM (left) and optical microscope (right) images of DNH fabricated in the gold film.

S2 Optical forces in confined fields

Forces in the dipole approximation: Conventional optical tweezers can be well described by the dipole approximation[1-5], where the particle dimension is much smaller than the illumination wavelength ($r_p << \lambda$). In this case, the particle is approximated by an electric dipole and two types of *time-averaged* optical forces can be considered[2, 4].

The first type of force, the *gradient force* due to dielectrophoresis, is proportional to the gradient of the square of the electric field, which pulls the particle towards the region of maximum light intensity. This term is called the optical trapping force and is a conservative force.

$$\left\langle \vec{F}_{grad} \right\rangle = \pi {r_p}^3 \varepsilon_0 n_f^2 \frac{n_p^2 - n_f^2}{n_p^2 + 2n_f^2} \nabla \left| \vec{E} \right|^2 \tag{1}$$

where r_p is the particle radius, ε_0 is the vacuum permittivity, n_f is the refractive index of the surrounding medium and n_p is the refractive index of the particle.

The second type of force, the non-conservative *scattering force*, proportional to the total cross-section of the particle, can be written as the sum of two contributions: a *radiation pressure force* that acts to push the particle in the direction of the Poynting vector, and a *spin curl force* associated with a non-uniform distribution of the spin density of the light field.

$$\left\langle \vec{F}_{scat} \right\rangle = \frac{\sigma}{2c} \mathrm{Re}(\vec{E} \times \vec{H}^*) + \sigma c \nabla \times (\frac{\varepsilon_0}{4\omega i} \vec{E} \times \vec{E}^*) \tag{2}$$

For a plane wave of intensity I_0 propagating in direction of $\vec{s}$, the spin curl force is zero and the scattering force on a *dielectric* particle is:

$$\left\langle \vec{F}_{scat} \right\rangle = \frac{128\pi^5 r_p^6}{3\lambda^4 c} (\frac{n_p^2 - n_f^2}{n_p^2 + 2n_f^2})^2 I_0 \vec{s} \tag{3}$$

where σ is the total cross-section of the particle, c is the light speed in vacuum, λ is the trapping laser wavelength and $\vec{s}$ is the unit propagation vector.

Forces beyond the dipole approximation: When a particle cannot be approximated as a dipole, the net force exerted on it can be determined by the Maxwell's stress tensor (MST).[3, 6, 7] MST analysis is a rigorous way of computing the optical force acting on an object. The total *time-averaged* electromagnetic force exerted on a particle interacting with an optical field is given by:

$$\left\langle \vec{F} \right\rangle = \int_{\partial V} \left\langle \vec{\vec{T}}(\vec{r},t) \right\rangle \bullet \vec{n}(\vec{r}) da \tag{4}$$

where $\vec{\vec{T}}(\vec{r},t)$ is called Maxwell's stress tensor (MST), $\vec{n}(\vec{r})$ is the unit vector perpendicular to the object surface ∂V, and da is an infinitesimal surface element. In Cartesian components, the MST reads as:

$$\vec{\vec{T}} = [\varepsilon_e \vec{E}\vec{E} + \mu_e \vec{H}\vec{H} - \frac{1}{2}(\varepsilon_e E^2 + \mu_e H^2)\vec{\vec{I}}] \tag{5}$$

where $\varepsilon_e = \varepsilon_0 \varepsilon_r$, $\mu_e = \mu_0 \mu_r$ are the permittivity and permeability of the surrounding medium respectively, ε_0 is the vacuum permittivity, μ_0 is the vacuum permeability, ε_r is the relative permittivity and μ_r is the relative permeability. The fields used to calculate the force are the self-consistent fields, which means that they are a superposition of the incident and the scattered fields. The trapping potential energy of the particle in the force fields can be directly defined as[3]:

$$U(\vec{r}_0) = -\int_{\infty}^{\vec{r}_0} \left\langle \vec{F}(\vec{r}) \right\rangle \bullet d\vec{r} \tag{6}$$

For comparison, we calculate the force on a NP (20 nm diameter) in the vicinity of the DNH structure using both the gradient force (dipole approximation) and the MST method (i.e. the rigorous approach). The configuration is schematically illustrated as Fig. S2a. The results are shown as Fig. S2b. It can be seen that the methods yield results that are in general agreement. This is reasonable because the NP is small (20 nm diameter) and has a refractive index that is close to that of the water. Accordingly, we employ the optical gradient force in the Langevin equation for the trajectory simulations.

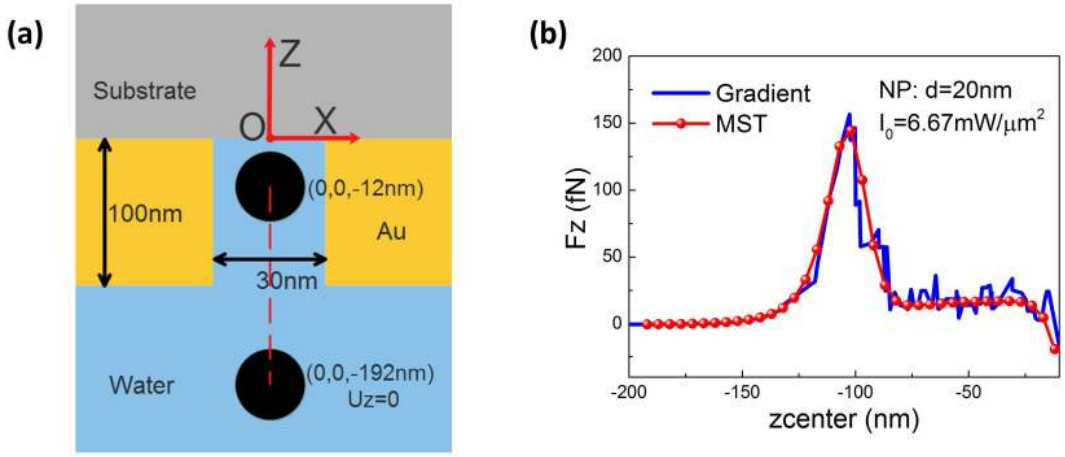

Figure S2. (a) Schematic diagram for MST force calculation. (b) Comparison of vertical force F_z along z direction exerted on a 20 nm polystyrene NP trapped by a DNH, calculated by the dipole approximation (Eq. 1) and the MST (Eq. 4) for I_0=6.67 mW/μm^2. (x_{center}=y_{center}=0)

S3 COMSOL simulation method

We use COMSOL Multiphysics to simulate our DNH with three-dimensional geometry.

S3.1 Numerical simulation of electromagnetic scattering, force and potential;

We use the "Wave Optics Module" of COMSOL Multiphysics. The DNH is formed in a 100 nm thick gold film on a glass substrate. The simulations are performed as follows. We begin by finding the background field ($|E_0|$) via a full-field simulation in which light is incident on the glass substrate from the water, i.e. the gold film and DNH are not included. We then perform a scattered-field simulation that includes the gold film and DNH. The first simulation is set up with two port conditions. One defines the incident plane wave and allows for reflection, while the other absorbs the transmitted plane wave. The side boundaries have Floquet periodicity conditions. The second simulation introduces DNH as the scatterer and surrounds the geometry with PMLs (perfectly matched layers).

To calculate the optical forces with the MST, as explained in Ref [8], the problem reduces to solving the electromagnetic scattering problem. In the scattered-field simulation, the DNH and a single NP are introduced as two scatterers. The results are shown as Fig. S3. Once the fields are found, the force acting on the NP surface is determined by the MST. To find the force maps, this process is repeated for different choices of the NP position (x, y, z). The trapping potential is

found from the force map using the COMSOL "PDE Module" (partial differential equations). The refractive indices of water, glass and polystyrene are taken as 1.33, 1.45 and 1.6 respectively. The optical constant of gold is taken from the data of Johnson and Christy [9] (i.e. relative permittivity at 1064 nm is ε_r=-48.45-*i*3.6).

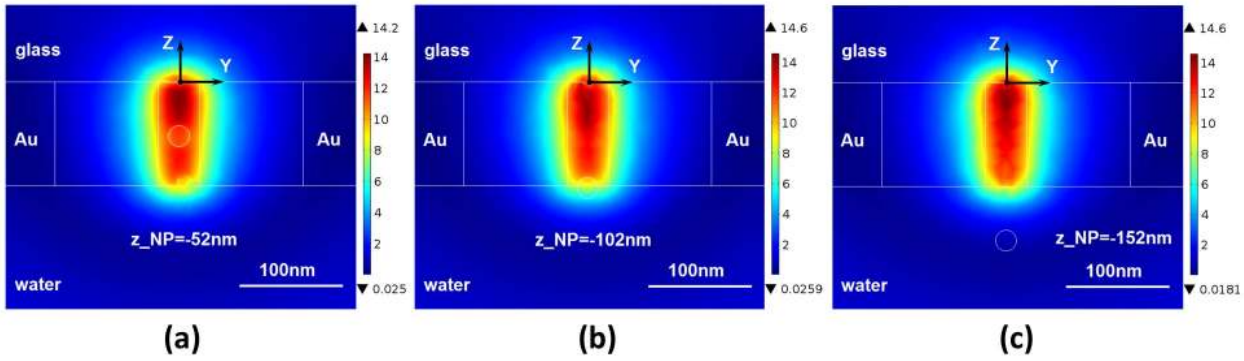

Figure S3. Electric field enhancement ($|E|/|E_0|$) distribution (x=0 cross section) in DNH, with a single NP (20 nm diameter) included in simulation. Plane wave illumination from water side is employed (x-polarized, λ=1064 nm). Black dot indicates coordinate system origin. Center z-coordinates of NP are as follows (with (x_{center}, y_{center})=(0 nm, 0 nm)). (a) z_{center}=-52 nm; (b) z_{center}=-102 nm; (c) z_{center}=-152 nm.

S3.2 Numerical simulation of thermal effects;

We use the heat transfer module ("Conjugate Heat Transfer-Laminar Flow") to solve the heat transfer and Navier-Stokes equations (here for steady state). The geometric configuration is shown in Fig. S4 (plot in y=0 and z=-50 nm cross section). The equations used in the modeling are as detailed in Ref [10-12], and include determination of the heat source, heat transfer in the solid and fluid regions, and non-isothermal flow in the water with volume force due to buoyancy. From the scattering simulation (Section S3.1), we can determine the absorbed total power from volume integration of power dissipation density. The spot size of the laser that is used in the experiments to illuminate the DNH is ~ μm-scale. We thus assume that the only source of heat in the system is the gold region with extent 1 μm×1 μm×100 nm that is centered over the DNH. We furthermore assume that the heating power is uniformly distributed throughout this region, which is reasonable because of the high thermal conductivity of gold. In the simulation, the outer glass boundaries are set to be 293.15 K. The initial temperature is also set to be 293.15 K. No-slip boundary conditions are employed at the boundaries between water and gold/glass. The

temperature-dependent thermal parameters of gold, glass and water are taken from COMSOL material library. The chamber height is taken to be 20 µm. As noted previously[10], the chamber height has an important influence on the magnitude of the water convection.

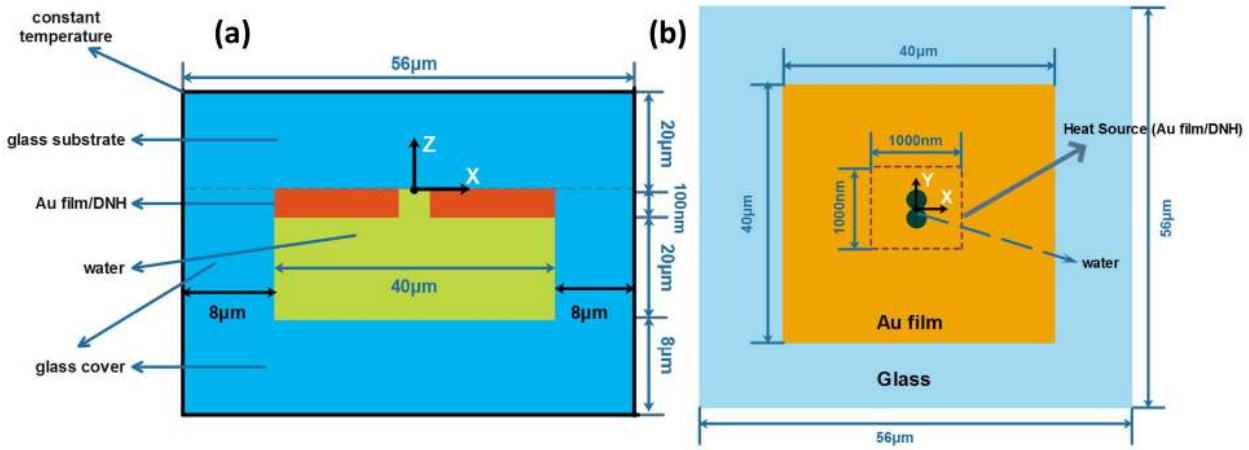

Figure S4. Geometric configuration used for the heating calculation. Sketch is not to scale. (a) *y*=0 cross section. Black line indicates chamber glass boundaries at which T_0=293.15 K. (b) *z*=-50 nm cross section. Purple dashed line indicates region that is assumed to act as the heat source.

The results of our heating calculations are shown as Fig. S5. These show the heat source power as a function of illumination intensity (Fig. S5a), the steady state temperature rise distribution (Fig. S5b) and the water convection velocity distribution in close proximity (200 nm, Fig. S5c) and further away (10 µm, Fig. S5d) from the gold film.

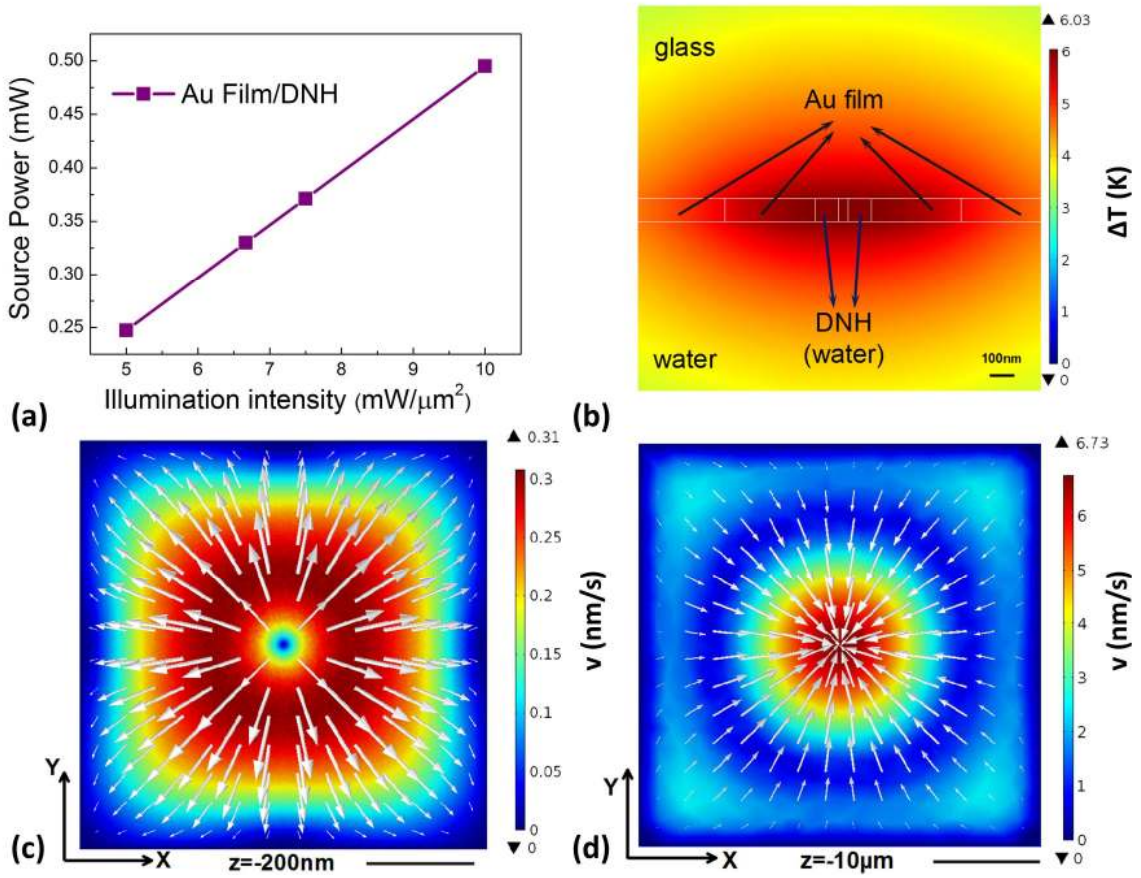

Figure S5. (a) Heat source power as a function of trapping laser intensity. (b) Steady-state temperature increase (ΔT: K) profile around DNH (x=0 cross section). (c)(d) FEM simulations of water convection velocity plotted in both magnitude (color map: nm/s) and direction (white arrows, magnitude proportionally-scaled). Scale bar: 10 μm. (c) z=-200 nm cross section; (d) z=-10 μm cross section. For panels b-d, I_0=6.67 mW/μm^2.

S3.3 Numerical simulation of particle trajectories;

We use the "Particle Tracing" option of the "Fluid Flow Module" of COMSOL Multiphysics to simulate particle trajectories. Initially (i.e. t=0), polystyrene nanospheres (20 nm diameter, n_{NP}=1.6) are released at different positions. For all of these, the initial velocities are zero. Forces on the particle include Stokes drag, gravity with buoyancy, Brownian and dielectrophoretic (i.e. optical gradient force) forces. We use the "Bounce" option of the module to model the interaction of the particle with the wall, i.e. the particles are taken as bouncing off the walls in a way that conserves particle momentum. This simplifying approach is often used when tracking particles in a fluid, but it may be interesting in the future to develop a more complex approach.

Stokes drag is used, with the background fluid velocity set to be zero. We make this assumption due to the fact that the modeling (e.g. Fig. S5c and d) reveals that it is very small. The basic form of Stokes drag (Eq. 2 of main text) is for the case of a sphere with a very small Reynolds number in an unbounded viscous fluid. If rather than being in an unbounded fluid, the sphere is close to a wall, then the Stokes drag is modified, as given by Faxén's law. We note however that the basic form of Faxén's law is only rigorously applicable to a much simpler geometry (sphere near flat wall) than our case (sphere inside or near DNH). We therefore employ Stokes drag in its basic form, and do not modify it via Faxén's law. For the dielectrophoretic force (optical gradient force) we use the electric field distribution found using the "Wave Optics Module", using piecewise polynomial recovery smoothing it to make results more accurate. The particle and water densities are 1.04 g/cm^3 and 1 g/cm^3 respectively. The temperature is set to be 300 K, which is roughly the sum of initial value 293.15 K and temperature increase ΔT at I_0=6.67 mW/μm^2. The water viscosity is 0.859 mPa·s. The time stepping method is the generalized-alpha method. The steps taken by solver are manually set to be 0.1 ns (*optical gradient force* only) and 0.5 ns (*all forces*). Data is extracted from the solver every 1 ns. In the simulation, a forward Euler step is used to compute the motion both before and after the wall collision when a particle-wall interaction happens.

S4 Optical force calculation using Maxwell stress tensor method

Calculations made using the Maxwell's stress tensor (MST) method of the force (F_z, i.e. vertical component) on the nanoparticle (NP) and the trapping potential energy U_z are shown as Fig. S6. It can be seen from Fig. S6a that F_z increases with the NP diameter, which is also expected from the dipole approximation. From Fig. S6b and c, it can be seen that F_z decreases with distance from the gold film surface and DNH, which is to be expected due to the evanescent nature of the fields. It can be seen from Fig. S6d that F_z is largest when the NP is close to the entry to the DNH. Calculations of trapping potential energy U_z and F_z are presented as Fig. S6e and f.

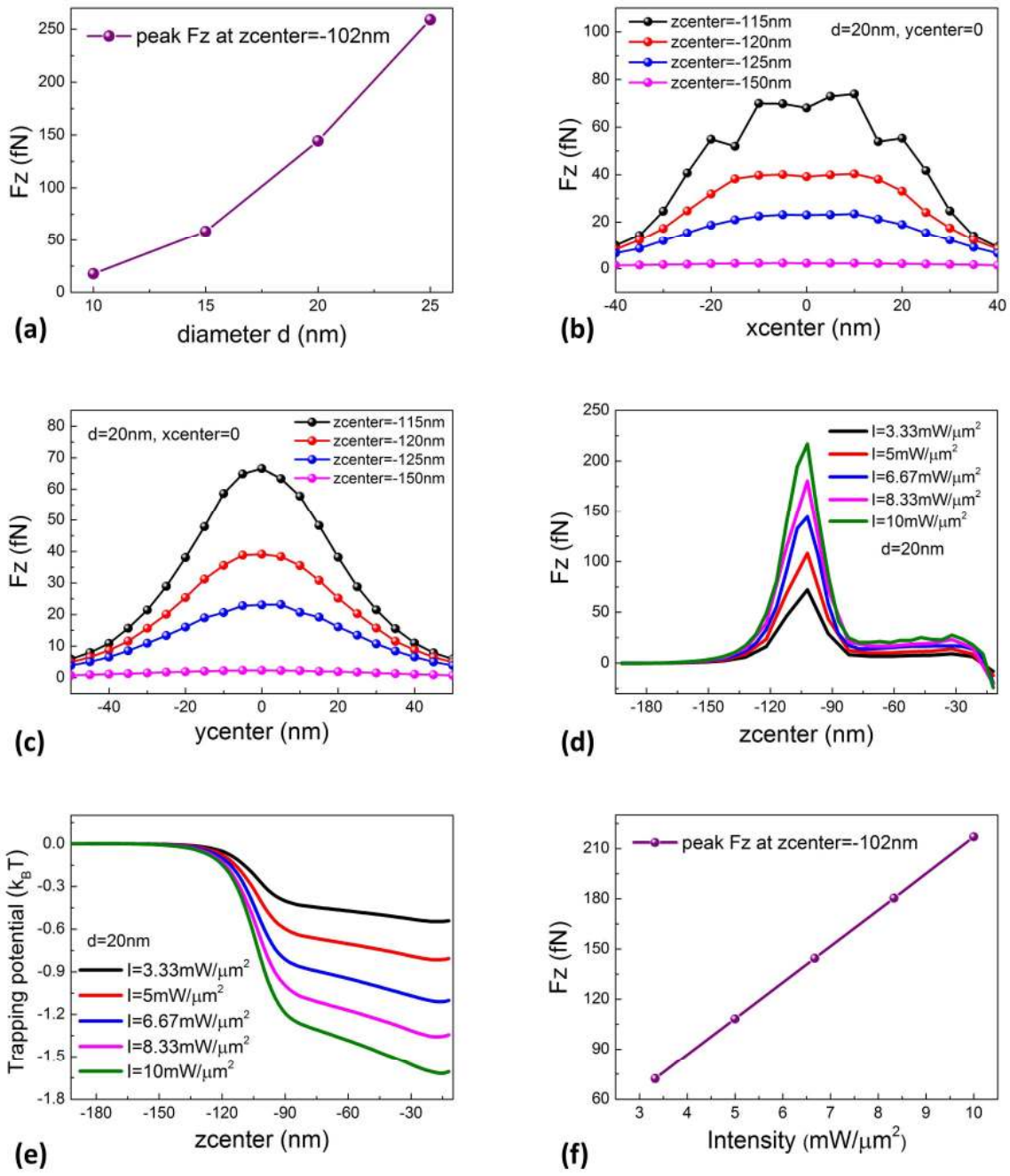

Figure S6. Optical forces of DNH exerted on a polystyrene nanoparticle (n_{NP}=1.6). (a) Peak F_z vs NP diameter d (extracted from data of Figure 3a). (b)(c) Vertical force F_z exerted on d=20 nm NP vs position. (b) y_{center}=0; (c) x_{center}=0. For panels a-c, I_0=6.67 mW/μm^2. (d) Vertical force F_z and (e) trapping potential energy U_z along z direction exerted on a 20 nm NP, as functions of

trapping laser intensity and position. (x_{center}=y_{center}=0) (f) Peak F_z vs trapping laser intensity (extracted from data of Figure S6d).

S5 EM-CCD fluorescence image of nanoparticles

As an additional check of the imaging capabilities of our system, we place a drop containing NPs at high concentration between two glass coverslips. This is then mounted in our optical microscope, and illuminated by our green laser. The image obtained with the EM-CCD camera is shown as Fig. S7a, with a red circle indicating an example of a single NP. We also use the system to obtain the fluorescence spectrum (Fig. S7b).

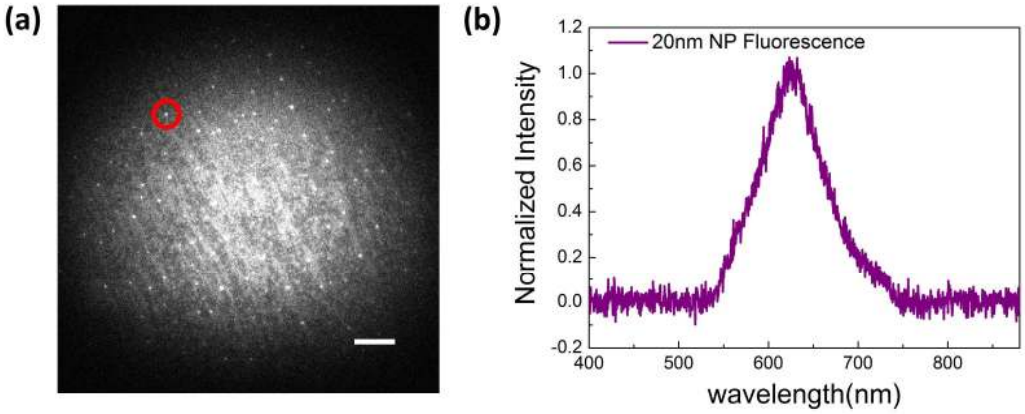

Figure S7. (a) EM-CCD image and (b) spectrum of high concentration NP solution drops between two coverslips, illuminated by a green laser. A single NP is indicated by a red circle. Scale bar: 8 μm.

S6 Results of numerical simulations of particle trajectories in DNH trapping

Selected results of the numerical simulations of the NP trajectory carried out using the method described in Section S3.3 are shown as Fig. S8. In Fig. S8a, simulated trajectories are presented in which the forces acting on the NP are due to the optical gradient force, gravity with buoyancy and Stokes drag (i.e. no Brownian force). In Fig. S8b, three particle trajectories are calculated with all forces in the *xz*-plane. In Fig. S8c and d, the results of ten simulated NPs trajectories (each with duration 100 μs) with all forces are shown as histograms in *x*- and *y*-axes. For panels a-d, I_0=6.67 mW/μm^2. In Fig. S8e, particle trajectories are plotted with all forces in the *xy*-plane. In Fig. S8f, a histogram of vertical NP positions with all forces is presented. For panels e and f, I_0=20 mW/μm^2.

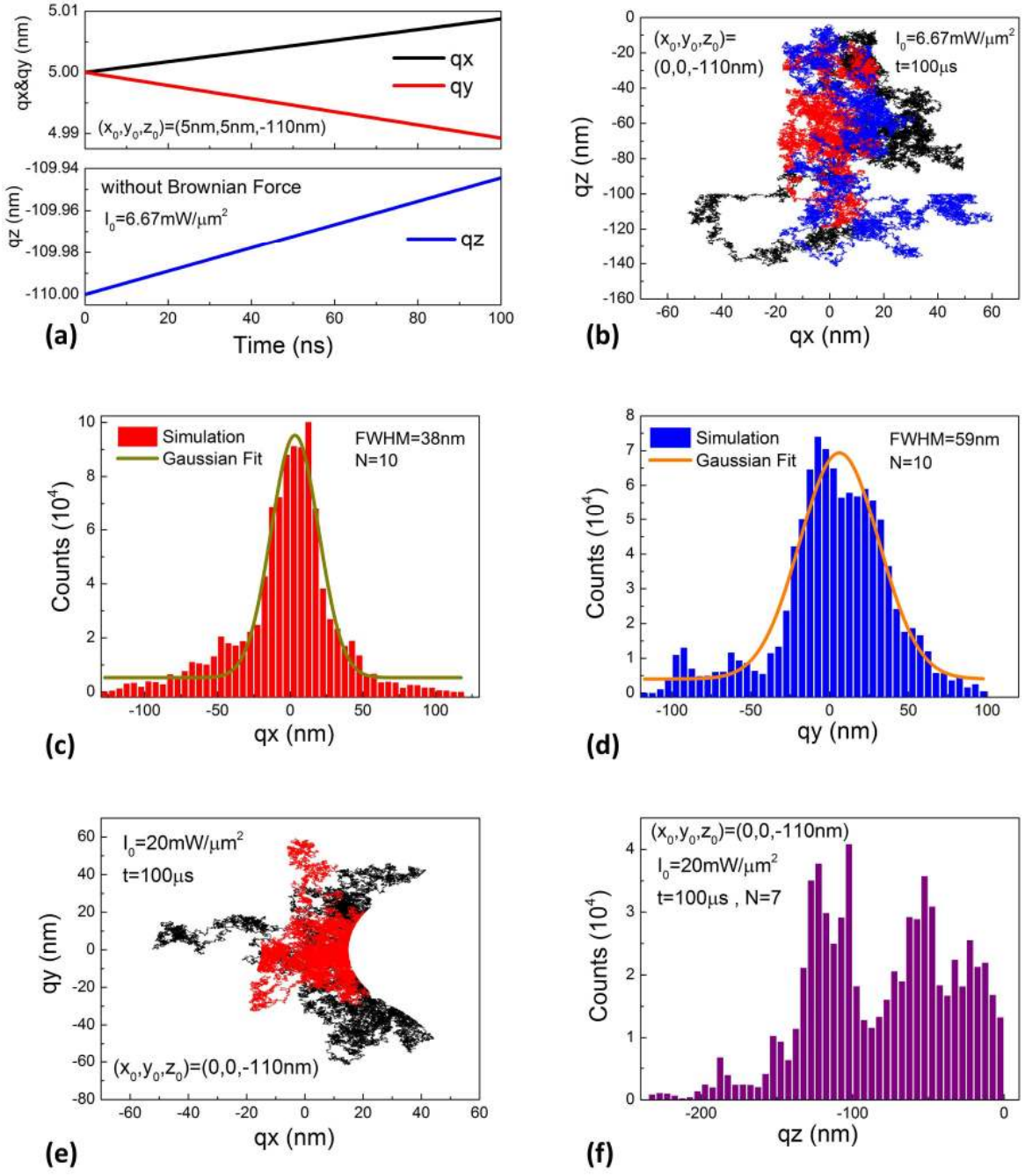

Figure S8. (a) Simulation of NP (20 nm diameter) trajectories influenced by drag force, gravity with buoyancy and optical force. (x_0,y_0,z_0)=(5 nm,5 nm,-110 nm). Trapping laser intensity I_0=6.67 mW/μm^2. Time step: 0.1 ns. (b)-(f) Simulation of particle trajectories (20 nm diameter) over 100 μs influenced by all forces. (x_0,y_0,z_0)=(0,0,-110 nm). Time step: 0.5 ns. (b) Position tracking in *xz*-plane for three NPs (same color particles as Figure 5d&e). Histograms of (c) *x*-

positions and (d) *y*-positions of ten NPs trajectories, for bin width of 5 nm (same ten NPs as Figure 5f). (e) Position tracking in *xy*-plane for two NPs. (f) Histogram of vertical positions of trajectories of seven modeled particles during 100 μs, for bin width of 5 nm. For panels b-d, I_0=6.67 mW/μm^2. For panels e&f, I_0=20 mW/μm^2.

Captions for Supporting Movies

Supporting Movie 1. DNH trapping and release of a single 20 nm polystyrene nanosphere. The movie is recorded at 30 fps. Trapping laser power P=38 mW (before objective) (i.e. I_0=16 mW/μm^2).

Supporting Movie 2. Optical tracking of a 20 nm nanoparticle trapped by a DNH. The movie is recorded at 30 fps. Trapping laser power P=15 mW (before objective) (i.e. I_0=6.6 mW/μm^2).

SUPPORTING INFORMATION REFERENCES

(1) Neuman, K. C.; Block, S. M. Optical trapping. *Rev. Sci. Instrum.* **2004**, 75, 2787-2809.
(2) Albaladejo, S.; Marqués, M. I.; Laroche, M.; Sáenz, J. J. Scattering forces from the curl of the spin angular momentum of a light field. *Phys. Rev. Lett.* **2009**, 102, 113602.
(3) Novotny, L.; Hecht, B. *Principles of Nano-Optics*. Cambridge University Press: **2012**.
(4) Spesyvtseva, S. E. S.; Dholakia, K. Trapping in a material world. *ACS Photonics* **2016**, 3, 719-736.
(5) Wang, K.; Crozier, K. B. Plasmonic trapping with a gold nanopillar. *ChemPhysChem* **2012**, 13, 2639-2648.
(6) Wang, X.; Wang, X. B.; Gascoyne, P. R. General expressions for dielectrophoretic force and electrorotational torque derived using the Maxwell stress tensor method. *J. Electrostatics* **1997**, 39, 277-295.
(7) Jackson, J. D. *Classical Electrodynamics*. John Wiley & Sons: **2007**.
(8) Ploschner, M.; Mazilu, M.; Krauss, T. F.; Dholakia, K. Optical forces near a nanoantenna. *J. Nanophotonics* **2010**, 4, 041570.
(9) Johnson, P. B.; Christy, R. W. Optical constants of the noble metals. *Phys. Rev. B* **1972**, 6, 4370-4379.
(10) Donner, J. S.; Baffou, G.; McCloskey, D.; Quidant, R. Plasmon-assisted optofluidics. *ACS Nano* **2011**, 5, 5457-5462.
(11) Roxworthy, B. J.; Bhuiya, A. M.; Vanka, S. P.; Toussaint, K. C., Jr. Understanding and controlling plasmon-induced convection. *Nat. Commun.* **2014**, 5, 3173.
(12) Ndukaife, J. C.; Kildishev, A. V.; Nnanna, A. G.; Shalaev, V. M.; Wereley, S. T.; Boltasseva, A. Long-range and rapid transport of individual nano-objects by a hybrid electrothermoplasmonic nanotweezer. *Nat. Nanotechnol.* **2016**, 11, 53-60.